INTERNATIONAL ATOMIC ENERGY AGENCY
UNITED NATIONS EDUCATIONAL, SCIENTIFIC AND CULTURAL ORGANIZATION
INTERNATIONAL CENTRE FOR THEORETICAL PHYSICS
I.C.T.P., P.O. BOX 586, 34100 TRIESTE, ITALY, CABLE: CENTRATOM TRIESTE
UNITED NATIONS INDUSTRIAL DEVELOPMENT ORGANIZATION
INTERNATIONAL CENTRE FOR SCIENCE AND HIGH TECHNOLOGY

SMR: 630/6

MINIWORKSHOP ON NONLINEARITY:
Dynamics of Surfaces in Nonlinear Physics

(13 - 24 July 1992)

"Scaling Relations in thermal Turbulence: The Aspect-Ratio Dependence"

presented by:

A. Libchaber
NEC Research Institute
4 Independence Way
Princeton, NJ 08540
U.S.A..

Scaling relations in thermal turbulence: The aspect-ratio dependence

Xiao-Zhong Wu and Albert Libchaber
The James Franck Institute, The University of Chicago, 5640 South Ellis Avenue, Chicago, Illinois 60637
and The Enrico Fermi Institute, The University of Chicago, 5640 South Ellis Avenue, Chicago, Illinois 60637
(Received 28 June 1991)

We report scaling relations of thermal turbulence in cells of aspect ratio 0.5, 1.0, and 6.7.

PACS number(s): 47.25.Qv

In a thermal convection experiment, there are three control parameters, the Rayleigh number R,

$$R=\frac{g\alpha\Delta L^3}{\nu\kappa}, \tag{1}$$

the Prandtl number $P=\nu/\kappa$, and the aspect ratio $\Gamma=D/L$ of the experimental cell. Here g is the gravitational acceleration, α the thermal expansion coefficient, Δ the temperature drop across the cell, D and L are the cell diameter and height, respectively, and ν and κ are the fluid kinematic viscosity and thermal diffusivity, respectively. In a series of papers [1–5] on convection in low-temperature helium gas, with P about constant, we have studied the scaling relations of hard turbulence as a function of R. In this paper, we present the aspect-ratio dependence of the measured scaling relations in three cells of aspect ratio $\Gamma=1.0$, 0.5, and 6.7. Since the aspect ratio 1.0 was the simplest geometry in which to study the turbulence, we first used a cell of 8.7 cm in diameter and height, in which the maximum R was 10^{12}. For higher R with a fixed diameter D (D is limited by the cryogenic Dewar size and the maximum heat flux reasonable at low temperature), a small-aspect-ratio cell has to be used. With a cell of height 40 cm and diameter 20 cm ($\Gamma=0.5$), the highest R (10^{15}) has been reached, using a new Dewar. Finally we studied the largest aspect-ratio cell compatible with this Dewar, diameter 20 cm and height 3 cm ($\Gamma=6.7$), the maximum R value being 10^{11}.

The experimental system has been detailed in previous papers [4–6]; here we only mention the key points. A cylindrical cell, filled with helium gas of various densities, is heated from below; its top plate is regulated at a temperature around 5 K. We have measured the heat-transfer efficiency (characterized by the Nusselt number N) and local temperature fluctuations. N is the heat Q actually transported by the gas, normalized by the heat $\chi\Delta/L$ that would be conducted (χ is the thermal conductivity). Local temperatures are measured with bolometers of 200-μm size at various points in the cell. Bolometers at the center of the cell measure the turbulent temperature fluctuations without direct influence from the large-scale flow. Pairs of bolometers at the midheight of the cell and various radial positions give information on the large-scale velocity and the effect of lateral boundaries.

From the studies in the aspect-ratio-1.0 cell of the Nusselt number N and analysis of local temperatures, we have discovered two distinct turbulence states, soft turbulence for $R<10^8$ and hard turbulence for $R>10^8$ [3]. The probability distribution function (PDF) for the temperature fluctuations at the center is Gaussian for soft turbulence and exponential for hard turbulence. Its rms value scales differently in the two regimes. The large-

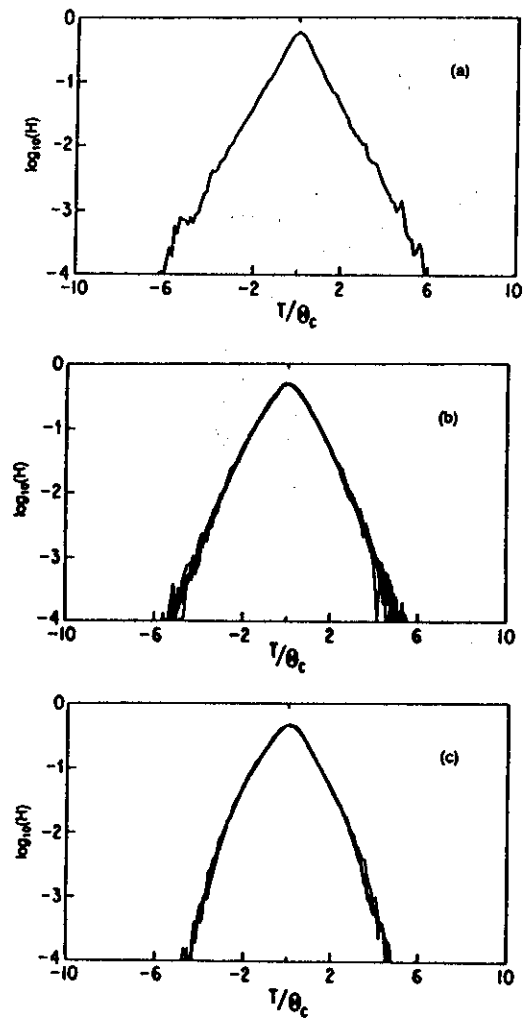

FIG. 1. The PDF in hard turbulence. (a) The PDF for $R=4\times10^{10}$ in the aspect-ratio-1.0 cell. Superposition of PDF for (b) $R=4\times10^9$, 7×10^{10}, 6×10^{11}, 7×10^{12}, 4×10^{13}, and 6×10^{14} in the aspect-ratio-0.5 cell, and (c) $R=2\times10^8$, 5×10^9, 2×10^{10} in the aspect-ratio-6.7 cell. The y coordinate is the logarithm of the probability, the x axis the linear temperature, in units of the individual rms value.

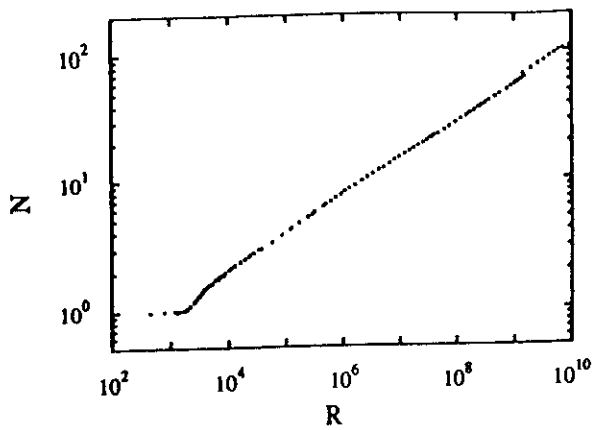

FIG. 2. The experimental N vs R for the cell of aspect ratio 6.7.

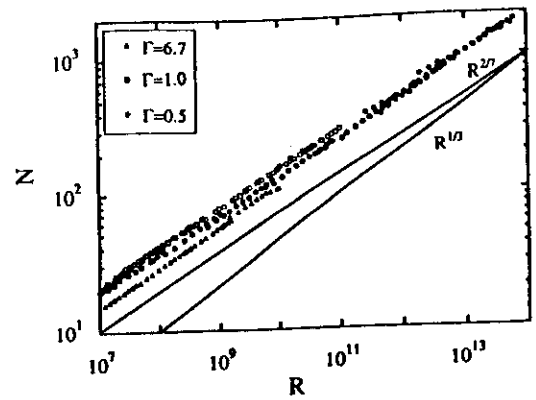

FIG. 3. For $R > 10^7$, the experimental N for the cells of aspect ratio 0.5 (filled circle), 1.0 (square), and 6.7 (triangle).

scale velocity measured by the side bolometers behaves differently in soft and hard turbulence. In hard turbulence, N scales with R with an exponent 0.285, different from the classical theory. The scaling relations in hard turbulence have been studied both experimentally and theoretically [4]. However, since the aspect ratio is a determining factor in thermal convection, together with R and P, it is interesting and necessary to check the aspect-ratio dependence of those behaviors. In this paper, we study the soft-turbulence–hard-turbulence transition in the three cells, then compare the scaling relations of hard turbulence.

One of the most important signatures of the transition is shown in the PDF of the temperature time series at the center of the cell. For $R < 4\times10^7$ in the aspect-ratio-1.0 cell in the soft-turbulence regime, it evolves from nonsymmetric to Gaussian, then to exponential; for $R > 4\times10^7$, hard turbulence, the PDF is exponential [Fig. 1(a)]. In the aspect-ratio-0.5 and -6.7 cells, the PDF changes similarly. For $R < 10^8$, they are neither invariant with R, nor symmetric. The asymmetry of the PDF indicates that the large-scale-flow structures are complex and nonergodic. As R increases, the PDF becomes less asymmetric. We speculate that while small-scale-flow structures are developing, the complex large-scale ones are gradually replaced by a simple one-roll circulation. For $R > 10^8$, the hard-turbulence regime, the PDF's are symmetric and remain invariant; they can be superposed after normalization by their rms values, as shown in Figs. 1(b) and 1(c).

The invariant and non-Gaussian PDF for $R > 10^8$ indicates that there is a hard-turbulence state in cells of aspect ratio ranging from 0.5 to 6.7 [7]. This invariance reflects the self-similarity of hard turbulence. The non-Gaussian shape implies correlations among motions of different scales. In the aspect-ratio-1.0 cell, the large-scale flow is steady, therefore the pure exponential PDF reflects the intrinsic correlations in hard turbulence. Nonsteady large-scale flow in the other two cells leads to a round tip. But even in this case, a high-pass filter applied to the time series will restore the exponential histogram, if the cutoff frequency corresponds to the cell circulation time. In other words, if we cut the nongeneric aspect of the large-scale flow, we recover an exponential histogram.

Now let us study the scaling relations of the Nusselt number N. The experimental N of the aspect ratio 6.7 is shown in Fig. 2. Heat transport is enhanced by the flow, so N becomes larger than 1 for $R > 1700$. For $R > 10^4$, it exhibits a power law with R,

$$N = 0.146R^{0.286\pm0.003} . \quad (2)$$

The scaling relation starts at $R = 10^4$, much before the soft-to-hard-turbulence transition $R = 10^8$. For the two other cells, N do not exhibit any power law until $R = 10^8$. To show the scaling region, N for the three cells are plot-

TABLE I. N for cells of different aspect ratios. Its value for each decade of R and its scaling relations are listed. The experimental sources are also provided.

P	R 10^5	10^6	10^7	10^8	10^9	10^{10}	Aspect ratio	$N = N(R)$	Source
0.7		7.14	14.1	27.7			1.5–4.4	$0.123R^{0.294}$	Goldstein and Chu [15]
Air			28.5	52.7	96.6	178	0.14	$0.398R^{0.265}$	Threlfall [1]
0.7							0.33	$0.328R^{0.257}$	Threlfall [1]
Helium		10.6	20.7	37.3	67.4	122	0.5	$0.165R^{0.291}$	Present work
			19.7	35.7	68.4	134	1.0	$0.217R^{0.285}$	Present work
	3.99	10.3	20.4	41.9	79.8	154	2.5	$0.173R^{0.280}$	Threlfall [2]
	4.35	8.28	15.8	30.1	57.3		6.7	$0.147R^{0.287}$	Present work
	4.00	7.83	15.0	28.9	56.0	109			

ted in Fig. 3. N for the aspect-ratio-1.0 cell can be fitted by

$$N = 0.22R^{0.285\pm0.004}, \quad (3)$$

while for the aspect ratio 0.5,

$$N = 0.17R^{0.290\pm0.005}. \quad (4)$$

From the fitting relations and Fig. 3, we can see that N in all the three cells have a consistent scaling exponent, but different prefactors.

These power laws, extending to the largest R reached, indicate that the flow is in a self-similar state in hard turbulence. In other words, the flow structures, such as the thermal boundary layers, the side-wall regions, etc., are invariant; only the time scale and length scale change with R.

The scaling exponents are all smaller than $\frac{1}{3}$, a theoretical value proposed by Malkus [8,9] and Howard [10]. They are consistent with $\frac{2}{7}$, proposed by Kadanoff and co-workers [4]. The $\frac{1}{3}$ relation has been supported by Townsend [11] and Goldstein and Tokuda [12]. But the range in Townsend's experiment was too small ($3\times10^8 < R < 7\times10^8$) to critically check the power law; the power law in Goldstein and Tokuda's experiment was deduced from cells of aspect ratio ranging from 0.57 to 4.5. Deardorff and Willis [13] have observed that N changes nonmonotonically with three aspect ratios, and reaches an asymptotic value for large aspect ratio. In Table I, the N value for each decade of R and its scaling relations for various aspect ratios are listed and they show similar aspect-ratio dependence. The asymptotic exponent value for large aspect ratio is 0.286, very close to $\frac{2}{7}$.

Now let us discuss the temperature fluctuations. Figure 4 shows, as a function of R, the rms value of the temperature fluctuations measured at midheight and various lateral positions in the aspect-ratio-1.0 cell. A turbulent flow has two competing effects on temperature fluctuations: first, it creates the fluctuations; on the other hand, it enhances mixing, thus reducing the temperature differences. The large-scale motion is more efficient in creating fluctuations and the small-scale ones are more

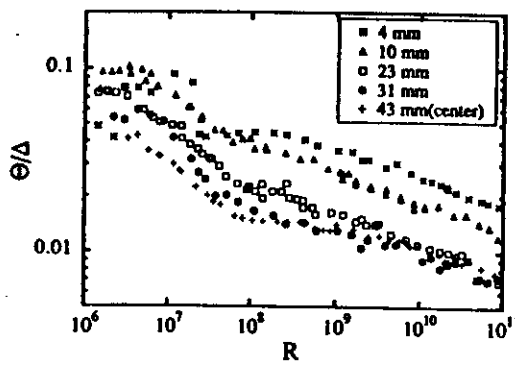

FIG. 4. The normalized rms temperature fluctuations Θ/Δ for various radial positions in the aspect-ratio-1.0 cell are plotted against R. Θ/Δ are measured at 4, 10, 24, 31, and 43 mm (center) away from the side wall.

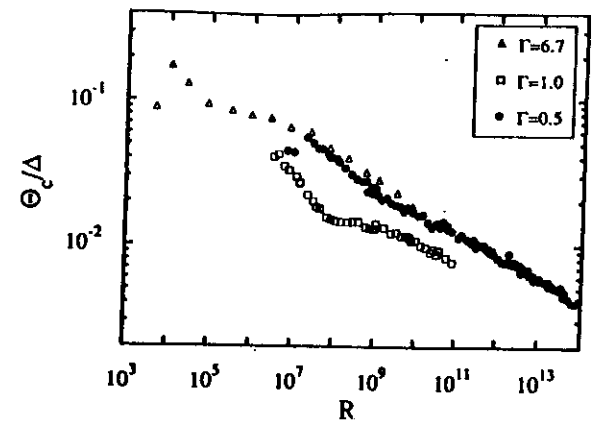

FIG. 5. The normalized rms temperature fluctuations Θ_c/Δ at the center of the cells of aspect ratio 0.5 (filled circle), 1.0 (square), and 6.7 (triangle).

efficient in mixing. For $R < 6\times10^6$, the temperature fluctuations increase with R, due to the building up of large-scale turbulent motion. For $R > 6\times10^6$, the rms value decreases with R; turbulent mixing is becoming dominant. The change of slope at $R = 4\times10^7$ indicates a change of turbulence structure: the soft-to-hard-turbulence transition.

For R above 4×10^7, the rms values have a power-law dependence with R (the scaling for the ones close to the center of the cell starts at R higher than 4×10^7). The scaling relation is

$$\frac{\Theta_c}{\Delta} = 0.23R^{-0.14\pm0.01}. \quad (5)$$

In Fig. 5, the rms temperature fluctuations at the center are plotted together, for the three cells. All of them show a change at $R \approx 10^8$, the point of soft-to-hard-turbulence transition. In the aspect-ratio-0.5 cell, Θ/Δ follows a power law for $R > 10^8$,

$$\frac{\Theta_c}{\Delta} = 0.46R^{-0.144\pm0.005}. \quad (6)$$

In the aspect-ratio-6.7 cell, not many data points have been taken to derive the rms value. Nonetheless, it displays a change at $R \approx 10^8$, and the scaling relation is

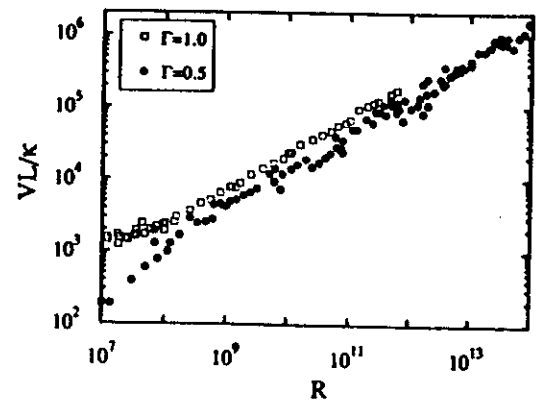

FIG. 6. The normalized velocity VL/κ of the aspect ratio 0.5 (filled circle) and 1.0 (square) cells.

TABLE II. The scaling relations in the three cells: $A \times R^{\gamma}$.

Aspect ratio		N	Θ_c/Δ	VL/κ
0.5	A	0.17	0.46	0.16
	γ	0.290±0.005	−0.144±0.005	0.49±0.02
1.0	A	0.22	0.23	0.31
	γ	0.285±0.004	−0.14±0.01	0.485±0.005
6.7	A	0.146	1.9	
	γ	0.286±0.003	−0.20±0.01	

$$\frac{\Theta_c}{\Delta} = 1.9R^{-0.20\pm0.01} . \tag{7}$$

In [4], where a model for hard turbulence has been proposed, an exponent $-\frac{1}{7}$ has been derived for the rms temperature fluctuation ($\frac{2}{7}$ for N). This value agrees with the experimental results in the aspect-ratio-0.5 and -1.0 cells quite well. The data in the aspect-ratio-6.7 yield a smaller slope, which needs more experimental points and larger R range to confirm.

The same theory in Ref. [4] predicted that the velocity fluctuations increase as $R^{3/7}$. Although we do not have an experimental technique to measure the fast velocity fluctuations, we have measured the large-scale flow via the correlation of two vertically spaced bolometers in the aspect-ratio-1.0 and -0.5 cells.

In the aspect-ratio-1.0 cell, the large-scale flow is found to be steady. The typical velocity in both cells is always of the order of 10 cm/sec. Figure 6 shows the normalized velocity VL/κ as a function of R. The soft-to-hard-turbulence transition is clear at $R = 4\times10^7$. In hard turbulence, the normalized velocity follows a power law

$$\frac{V}{\kappa/L} = 0.31R^{0.485\pm0.005} . \tag{8}$$

In this cell, such a steady large-scale flow creates a resonant peak at the circulation frequency f_p, which appears in signals of all parts of the cell [3,5].

In the aspect-ratio-0.5 cell, the large-scale velocity switches direction from time to time, but it still has one characteristic value. The resonant frequency is absent in this cell. The normalized velocity VL/κ is plotted as a function of R in Fig. 6(a). For $R > 1\times10^8$, the velocity has a scaling relation with R for $R > 10^8$,

$$\frac{V}{\kappa/L} = 0.16R^{0.49\pm0.02} . \tag{9}$$

The change at $R = 10^8$ [Fig. 6(b)] corresponds to the soft-to-hard-turbulence transition.

The scaling exponents for the velocity differ from the theoretical value $\frac{1}{2}$. In a theory proposed by Shraiman and Siggia [14], a logarithmic correction has been added to the velocity,

$$\frac{V}{\kappa/L} = 0.14P^{2/7}R^{3/7}[2.5\ln(VL/\nu)+6] , \tag{10}$$

which compensates for the difference [6].

Conclusion: The soft-to-hard-turbulence transition discovered in an aspect-ratio-1.0 cell is present in the cells with aspect ratio 0.5 and 6.7 at $R \approx 10^8$ as well [16–19]. In hard turbulence, the PDF is invariant and non-Gaussian; the Nusselt number N, the rms temperature fluctuation Θ_c/Δ, and the velocity VL/κ have simple scaling relations, which are summarized in Table II.

This research has been supported by the National Science Foundation under Contract No. DMR 8722714.

[1] D. C. Threlfall, Ph.D thesis, University of Cambridge, 1974 (unpublished).
[2] D. C. Threfall, J. Fluid Mech. 67, 17 (1975).
[3] F. Heslot, B. Castaing, and A. Libchaber, Phys. Rev. A 36, 5870 (1987).
[4] B. Castaing, G. Gunaratne, F. Heslot, L. Kadanoff, A. Libchaber, S. Thomae, X. Z. Wu, S. Zaleski, and G. Zanetti, J. Fluid Mech. 204, 1 (1989).
[5] M. Sano, X. Z. Wu, and A. Libchaber, Phys. Rev. A 40, 6421 (1989).
[6] X. Z. Wu, Ph.D. thesis, University of Chicago, 1991 (unpublished).
[7] G. S. Charlson and R. L. Sani, J. Fluid Mech. 71, 9175 (1975).
[8] W. V. R. Malkus, Proc. R. Soc. London, Ser. A 225, 185 (1954).
[9] W. V. R. Malkus, Proc. R. Soc. London, Ser. A 225, 196 (1954).
[10] L. N. Howard, in *Applied Mechanics, Proceedings of the 11th International Congress of Applied Mechanics, Munich (Germany)*, edited by H. Gortler (Springer, Berlin, 1966).
[11] A. A. Townsend, J. Fluid Mech. 5, 209 (1959).
[12] R. J. Goldstein and S. Tokuda, Int. J. Heat Mass Transfer 23, 738 (1980).
[13] J. W. Deardorff and G. E. Willis, J. Fluid Mech. 23, 337 (1965).
[14] B. I. Shraiman and E. D. Siggia, Phys. Rev. A 42, 3650 (1990).
[15] R. J. Goldstein and T. Y. Chu, Prog. Heat Mass Transfer 2, 55 (1969).
[16] H. T. Rossby, J. Fluid Mech. 36, 309 (1969).
[17] A. M. Garon and R. J. Goldstein, Phys. Fluids 16, 1818 (1973).
[18] T. Y. Chu and R. J. Goldstein, J. Fluid Mech. 60, 141 (1973).
[19] H. Tanaka and H. Miyata, Int. J. Heat Mass Transfer 23, 1273 (1980).